


Glycerol-mediated synthesis of monodisperse sub-10 nm selenium nanoparticles: An eco-friendly and sustainable route

Van-Lam Le^{1,2}, Thanh-Binh Huynh^{1,2}, Hoa-Hung Lam^{1,2},
Minh-Tam K. Nguyen^{1,2}, Trung Dang-Bao^{1,2*} 

¹ Faculty of Chemical Engineering, Ho Chi Minh City University of Technology (HCMUT), 268 Ly Thuong Kiet Street, Dien Hong Ward, Ho Chi Minh City, Vietnam

² Vietnam National University Ho Chi Minh City, Linh Xuan Ward, Ho Chi Minh City, Vietnam

* Corresponding author's e-mail: dbtrung@hcmut.edu.vn

ABSTRACT

This work reports a simple and green approach for synthesizing selenium nanoparticles (SeNPs) dispersed in glycerol, using ascorbic acid as a reducing agent. The formation of SeNPs in glycerol was monitored by Ultraviolet visible spectroscopy (UV-vis), while the characteristics of SeNPs were provided by X-ray diffraction (XRD), Fourier transmission infrared spectroscopy (FT-IR), energy dispersive X-ray (EDX) mapping analysis, and high-resolution transmission electron microscopy (HR-TEM). The zero-valent SeNPs were spherical and remarkably small, averaging 3.9 nm in diameter. Significantly, the colloidal SeNPs solution in glycerol exhibited stability for at least two months without any aggregation signs, a stark contrast to selenium precipitated in water. A comparative study with other polyols (ethylene glycol and propylene glycol) identified glycerol as uniquely effective, likely because its supramolecular structure promotes superior SeNPs dispersion. The glycerol-dispersed SeNPs demonstrated significant inhibitory efficacy against the growth of both *S. aureus* and *E. coli* bacteria. This finding suggests their substantial potential for diverse applications in antibacterial and biomedical domains.

Keywords: selenium nanoparticles, glycerol, eco-friendly and sustainable synthesis, antibacterial.

INTRODUCTION

The foundation of nanotechnology lies in the distinct physical characteristics, notably surface and size effects, that manifest when materials are reduced to nanometer dimensions. These effects provide the basis for the development of nanomaterials, among which metal nanoparticles represent a prominent system demonstrating numerous enhanced applications over larger-sized materials (Jamkhande et al., 2019). In the literature, silver nanoparticles have been extensively investigated for various applications such as sensing (Dang-Bao et al., 2023), catalysis (Thach-Nguyen et al., 2022; Ly et al., 2024), antibacterial (Phan et al., 2024; Nguyen et al., 2025), and biomedicine. Conversely, recent studies have also raised concerns that these materials may induce uncontrolled cytotoxicity and oxidative stress, especially when employed

at high doses or when accumulating in the body over extended periods (Tripathi et al., 2022). More recently, selenium nanoparticles (SeNPs) demonstrate the capacity to maintain or even augment antioxidant, anti-inflammatory, and immunomodulatory activities while concurrently exhibiting significantly reduced toxicity compared to conventional metal counterparts. Owing to their superior safety profile, precise dose control, and notable therapeutic efficacy, SeNPs are progressively garnering interest as a versatile material platform within the biomedical domain, particularly in the advancement of therapeutics for cancer treatment, anti-inflammatory interventions, and immunomodulation (Ferro et al., 2021; Karthik et al., 2024). Nevertheless, the biological efficacy of SeNPs is intrinsically linked to their synthesis methodology, which, in turn, dictates their resultant size, shape, and stability (Bisht et al., 2022; Huang et al., 2023).

Synthetic methods for SeNPs primarily include chemical and biological approaches (Xiao et al., 2023). Among these, chemical methods are widely employed due to their simple process, low cost, and ability to control particle morphology. However, a significant drawback is the environmental pollution caused by toxic reducing agents and the generation of harmful by-products. In contrast, biological methods, frequently referred to as “green” synthesis, employ microorganisms (e.g., bacteria, fungi) or plant extracts for the biosynthesis of SeNPs. This constitutes an environmentally benign approach that concurrently leverages the inherent biosynthetic capacity of biological systems to generate nanoparticles exhibiting elevated biological activity. Nevertheless, constraining factors, specifically protracted synthesis durations, inconsistent yields, and inherent difficulties in particle size regulation, impede the widespread practical implementation and large-scale production of this methodology.

From the discussed methodologies, the polyol method distinguishes itself as a highly promising approach for the synthesis of nanomaterials. Polyols possess the unique ability to concurrently act as solvents, reducing agents, and capping agents, thus facilitating meticulous control over particle nucleation and growth while simultaneously mitigating aggregation (Dang-Bao et al., 2021). This versatile technique has been successfully employed in the fabrication of diverse nanomaterials, such as silver nanoparticles (Nguyen et al., 2025), copper nanoparticles (Dang-Bao et al., 2022), and platinum nanoparticles (Tran et al., 2025), consistently demonstrating narrow size distributions and remarkable stability. Consequently, by effectively integrating the benefits inherent to both chemical and biological synthesis routes, the polyol method is increasingly recognized as a preeminent strategy in the field of nanomaterial synthesis, particularly in the context of developing safe and efficacious biomedical applications.

Herein, we report a simple and green approach for synthesizing SeNPs dispersed in glycerol, using ascorbic acid as a reducing agent. Within the class of polyol solvents, glycerol is particularly noteworthy, owing to its exceptionally favorable properties for the synthesis of nanomaterials, encompassing its elevated viscosity, high boiling point, non-volatile nature, inherent non-toxicity, and recognized safety profile for both pharmaceutical and food-grade applications (Dang-Bao et al., 2021). Given its

inherent ability to function concurrently as a solvent and a stabilizing agent, glycerol enables meticulous control over particle dimensions, effectively mitigates agglomeration, and substantially augments the dispersion stability of SeNPs within liquid matrices.

EXPERIMENTAL

Synthesis of SeNPs in glycerol

SeNPs were synthesized via the chemical reduction of sodium selenite (Na_2SeO_3) in glycerol, using ascorbic acid (AA) as a reducing agent. In a typical procedure, 20 mL of a glycerol solution containing 1 mM Na_2SeO_3 and 20 mM AA was magnetically stirred at 70 °C for 30 min. During this process, the solution transitioned from colorless to red, indicating the reduction of selenite (SeO_3^{2-}) to Se(0) and the subsequent formation of SeNPs.

The effects of various reaction conditions on SeNPs formation in glycerol were examined involving reaction time (up to 40 min), temperature (50–80 °C), and the molar ratio of Na_2SeO_3 -to-AA (from 1/15 to 1/25). To specifically investigate the influence of different polyols on SeNPs formation, this synthesis procedure was also performed under optimal conditions, with glycerol systematically replaced by water, ethylene glycol, and propylene glycol, respectively.

Upon completion of the reaction, the solution was cooled to room temperature and stored under ambient conditions for subsequent analysis. For solid SeNPs, the particles were separated by centrifugation, washed multiple times with distilled water and acetone, and then air-dried overnight.

Characterization of SeNPs

UV-Vis spectroscopy was employed to monitor the formation of SeNPs in glycerol. Absorbance scans were performed from 300 to 800 nm using an Optizen Pop spectrophotometer and a 1 cm-path length quartz cuvette. XRD was utilized to characterize the crystalline structure of the as-prepared solid SeNPs. Measurements were performed on a D2 Bruker diffractometer, employing Cu-K α radiation ($\lambda = 1.5406 \text{ \AA}$) within a 2θ range of 20–80°. FT-IR spectroscopic data were acquired on a Bruker-Tensor 27 instrument, with scans performed from 500 to 4000 cm^{-1} via the

KBr pellet method. HR-TEM imaging and SAED analysis were conducted on a JEOL JEM-2100 instrument to obtain high-resolution images and corresponding electron diffraction patterns.

Antibacterial activity of SeNPs in glycerol

The antibacterial activity of SeNPs dispersed in glycerol against (+) *S. aureus* and (–) *E. coli* was evaluated using the colony-forming unit (CFU) method as per our previous report (Phan et al., 2023). First, the SeNPs-glycerol solution was diluted in Mueller Hinton Broth (MHB). Bacterial suspensions were then added to the diluted SeNPs samples to achieve a final concentration of approximately 2×10^7 CFU/mL. These mixtures were cultured at 37 °C with shaking at 200 rpm for 3, 6, and 24 h. A control group, consisting of bacteria at a similar initial density, was cultured under identical conditions in MHB medium containing 50% (v/v) glycerol. At each predetermined time point (3, 6, and 24 h), the bacterial density in both the test and control samples was determined by spreading aliquots onto Petrifilm® Aerobic count plates. These plates were then incubated at

37 °C for 16 h. Following incubation, the number of CFUs on each film was counted, and the bacterial density in the original sample was calculated.

RESULTS AND DISCUSSION

Effect of reaction conditions on SeNPs formation in glycerol

The formation of SeNPs in glycerol over time, synthesized with AA as a reducing agent (Na_2SeO_3 -to-AA molar ratio of 1/20) at 70 °C, was characterized by UV-Vis spectroscopy and visual assessment of the solution's temporal color evolution (Figure 1a). Initially, the glycerol solution containing the Na_2SeO_3 precursor was colorless; as the reaction progressed, the reaction solution gradually turned red. This color change signifies the reduction of selenite ions (SeO_3^{2-}) to Se(0) and the subsequent formation and increasing concentration of SeNPs (Ranjitha and Rai, 2022; Abdelsalam et al, 2023). Concurrently, UV-Vis spectra revealed a broad absorption peak with a maximum (λ_{max}) at approximately 600–620 nm,

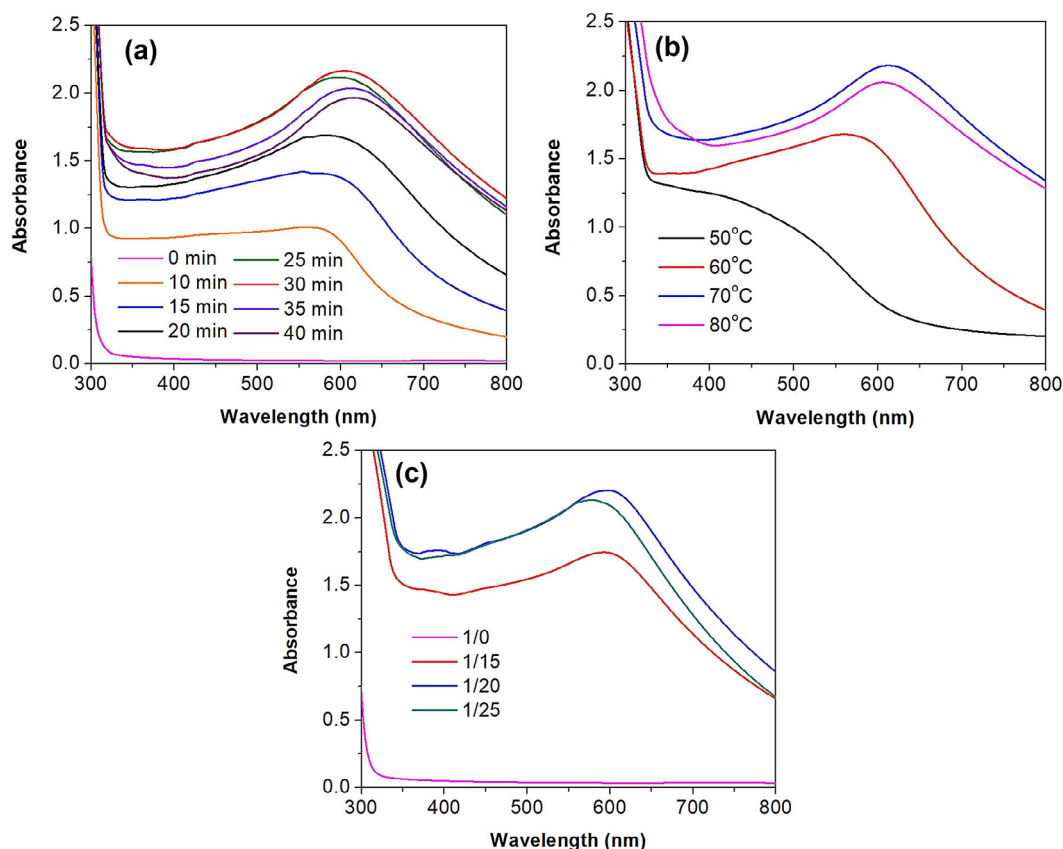


Figure 1. UV-Vis spectra of SeNPs in glycerol under various reaction conditions: (a) time, (b) temperature, and (c) Na_2SeO_3 -to-AA molar ratio

characteristic of the surface plasmon resonance (SPR) of SeNPs (Mollania et al., 2016; Ullah et al., 2021). The intensity of this absorption peak steadily increased over time. At 30 min, the absorption peak became more symmetrical with a stable amplitude, approaching saturation. This indicates that the SeNPs formation rate had reached its peak, and the colloidal system achieved significant stability. Beyond the 30-min mark, the λ_{\max} position exhibited a red shift (shifting towards longer wavelengths), and the absorption peak intensity decreased. This spectroscopic change suggests an increase in particle size. Consequently, 30 min was determined to be the optimal reaction time, as the solution achieved a stable red color and the absorption spectrum displayed a distinct, saturated peak, signifying complete SeNPs formation and optimal colloidal system stability.

The UV-Vis spectra recorded across the investigated temperature range of 60–80 °C consistently displayed a maximum absorption peak at 600–620 nm, which is characteristic of the SPR of spherical SeNPs (Figure 1b). In contrast, at 50 °C, the absorption spectrum was notably weak and steep. This suggests a slower reduction reaction and lower particle formation efficiency. The sample reacted at 70 °C yielded the highest absorbance at 615 nm, exhibiting a sharp and symmetric peak shape. This indicates the formation of high-density particles and a stable colloidal system. At 80 °C, while an absorption peak was still present, its intensity decreased compared to that at 70 °C, and the peak broadened. This broadening suggests the possibility of larger particles or agglomeration occurring at this higher temperature.

In terms of reaction kinetics, as temperature rises, the rate of selenite ions (SeO_3^{2-}) reduction to $\text{Se}(0)$ accelerated due to increased kinetic energy (Mollania et al., 2016; Puri et al., 2024). This rapid nucleation led to a greater number of nanoparticles and, consequently, a higher optical density at λ_{\max} . However, once the temperature surpassed the optimal level (at 80 °C in this case), the elevated kinetic energy caused the still-forming, unstable particles to collide and aggregate more frequently. This led to an increase in particle size, a decrease in absorption intensity, and a red shift in λ_{\max} . Therefore, the optimal reaction temperature was 70 °C, ensuring that the selenium nucleation reaction took place with high efficiency, the nanoparticles were stable and well dispersed.

Similarly, the UV-Vis spectra recorded at various Na_2SeO_3 -to-AA molar ratios (1/15, 1/20, and

1/25) all displayed a maximum absorption peak between 600–620 nm (Figure 1c). This is the characteristic absorption for the SPR of SeNPs. However, in the absence of AA (at a ratio of 1/0), no such absorption peak appeared, confirming that SeNPs formation did not occur.

The ratio of 1/20 yielded the highest absorption peak. This indicates that this specific amount of AA was sufficient to ensure the complete reduction of selenite ions (SeO_3^{2-}) to $\text{Se}(0)$. It also suggests that the AA promptly stabilized the nanoparticle surfaces immediately after formation, which helped reduce secondary agglomeration. At a lower AA concentration (a ratio of 1/15), the reduction process was incomplete, leading to fewer SeNPs. Additionally, the colloidal system was prone to agglomeration due to insufficient surface protection. Conversely, at a higher AA concentration (a ratio of 1/25), a decrease in the absorption peak was observed, likely due to increased shielding and background scattering effects caused by the excess AA.

To sum up, the synthesis of SeNPs in glycerol were optimized with the following conditions: a reaction time of 30 min, a temperature of 70 °C, and a Na_2SeO_3 -to-AA molar ratio of 1/20.

Effect of glycerol on SeNPs immobilization and stability

The crucial role of glycerol in SeNPs synthesis was explored, identifying it as both a solvent and a stabilizing/immobilizing agent. Glycerol's unique attributes, including its substantial viscosity (approximately 1410 mPa·s at 25 °C), high polarity, and the presence of three hydroxyl groups, are instrumental in stabilizing SeNPs. These properties facilitate stabilization through hydrogen bonding and electrostatic interactions. Additionally, glycerol's high viscosity effectively retards the agglomeration rate, promoting uniform particle growth and excellent dispersion (Dang-Bao et al., 2022; Nguyen et al., 2025).

To investigate the impact of different solvents, we synthesized SeNPs under optimal conditions in glycerol (GL), ethylene glycol (EG), propylene glycol (PG), and water (WT). The UV-Vis spectra of the resulting SeNPs solutions (Figure 2a) revealed a clear distinction: only the glycerol-dispersed SeNPs exhibited an absorption peak at 615 nm, characteristic of their SPR. In stark contrast, the absorption spectra for solutions prepared with EG, PG, and WT showed no such peak, indicating

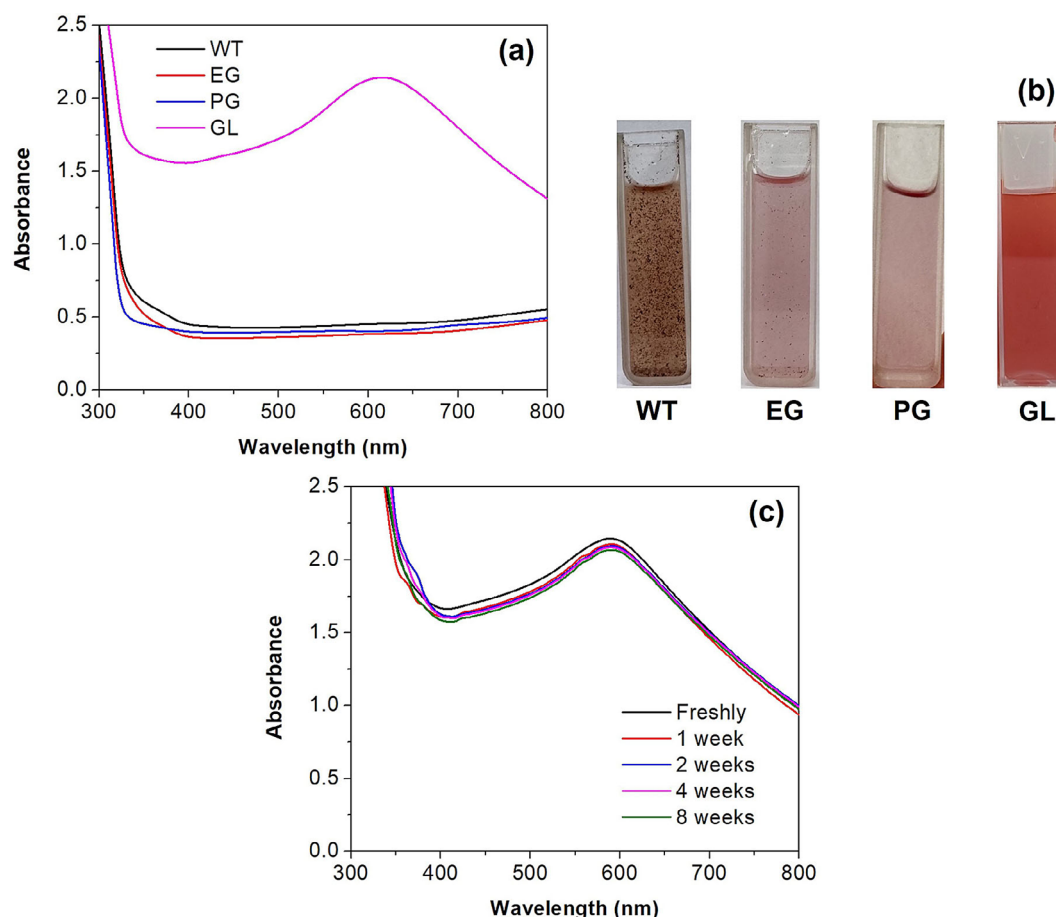


Figure 2. (a) UV-Vis spectra and (b) photos of SeNPs in various solvents, (c) UV-Vis spectra of SeNPs in glycerol over 8 weeks of ambient storage

low nanoparticle formation efficiency and unstable colloidal systems. This spectroscopic evidence was consistent with our visual observations (Figure 2b): the glycerol-based solution was transparent and red, while the others displayed uneven sedimentation or precipitation, further confirming glycerol's superior role in SeNPs synthesis and stabilization. Compared to EG and PG, glycerol stands out due to its longer carbon chain and higher number of hydroxyl groups. These features enable glycerol to form a more efficient supramolecular network, which in turn allows for better trapping of SeNPs within the solution (Dang-Bao et al., 2022; Nguyen et al., 2025).

The excellent colloidal stability of SeNPs synthesized in glycerol under optimal conditions was confirmed by monitoring their UV-Vis spectra over 8 weeks of ambient storage (Figure 2c). A distinct absorption peak between 600–620 nm remained present in all spectra. While a minor reduction in λ_{max} absorption intensity was noted over time, this alteration was negligible across the 8-week duration, with peaks retaining their symmetrical

form and stable amplitude. This lack of significant change demonstrates that no substantial nanoparticle aggregation occurred during storage.

Characteristics of SeNPs in glycerol

The crystalline structure of the solid SeNPs was confirmed by XRD analysis (Figure 3a). The observed diffraction peaks aligned perfectly with the (100), (101), (110), (102), (111), (201), (112), and (202) planes of hexagonal selenium (JCPDS 06-0362) (Lian et al., 2019). Furthermore, the lack of any characteristic peaks corresponding to selenium dioxide demonstrated that only zero-valent SeNPs were present. Crystallite size analysis of the SeNPs, derived from the (101) diffraction peak utilizing the Scherrer equation, yielded a value of 29.6 nm. It is imperative to acknowledge that the XRD measurements were conducted on solid-state SeNPs, which were isolated from their colloidal dispersion by centrifugation. The subsequent removal of stabilizing agents, specifically ascorbic acid and glycerol,

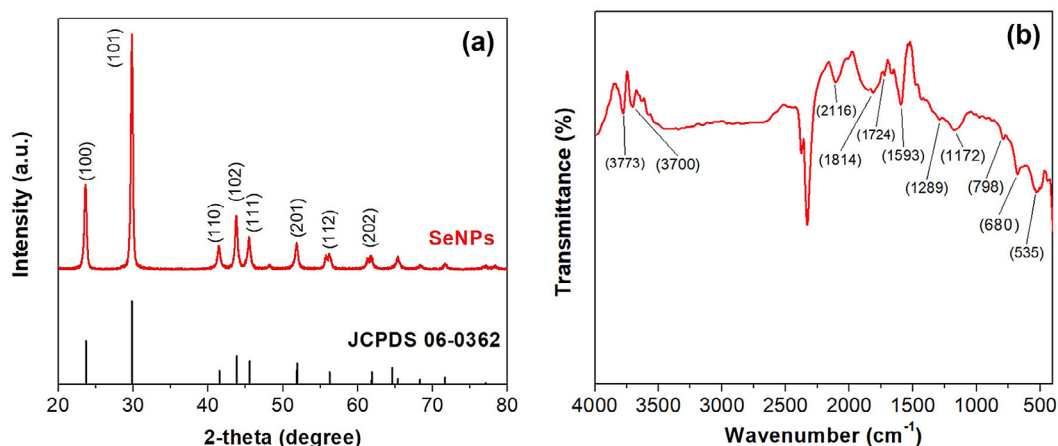


Figure 3. (a) XRD and (b) FT-IR analysis of solid SeNPs

during this isolation process induced nanoparticle agglomeration. This observed agglomeration provides a plausible explanation for the discrepancy between the XRD-derived crystallite size and the smaller particle dimensions obtained from direct measurements of SeNPs in their liquid-phase glycerol suspension (HR-TEM analysis). These observations underscore the critical stabilizing function of glycerol in mitigating the agglomeration and precipitation of SeNPs, phenomena that would otherwise lead to an undesirable increase in effective particle size.

The FT-IR spectrum of the solid SeNPs provided clear evidence of functional groups integral to their synthesis and stabilization (Figure 3b). The signals observed at 680 cm⁻¹ and 535 cm⁻¹ were attributed to Se–Se vibrational modes within the hexagonal phase selenium crystal lattice. Characteristic peaks at 3773 cm⁻¹ and 3700 cm⁻¹ corresponded to free hydroxyl (–OH) groups, indicating the presence of glycerol molecules on the nanoparticle surface that contribute to SeNPs dispersion and chemical stability. Prominent peaks located at 2116 cm⁻¹, 1814 cm⁻¹ and 1724 cm⁻¹ were assigned to carbonyl (C=O), being consistent with the reduction of selenite ions and the generation of aldehyde and ketone by-products. Furthermore, signals at lower wavenumbers, including 1593, 1289, 1172, and 798 cm⁻¹, represented stretching and bending vibrations of C=C, C–O, C–O–C, and hydrocarbon groups, indicative of the complex organic coating (Siddique et al., 2024). Collectively, these functional groups serve to prevent SeNPs agglomeration and improve their interfacial interactions, thereby enhancing their utility in diverse biological and industrial applications.

Quantitative analysis via EDX spectroscopy (Figure 4a) on the solid SeNPs sample indicated a substantial selenium content, evidenced by a highly intense signal corresponding to an estimated 88.38 mass% of the element. This compositional data strongly supported the conclusion that the synthesized material was predominantly elemental selenium. The exceptionally low background intensity surrounding the selenium peak further confirmed high purity and the negligible formation of selenium oxide (SeO_x), which typically manifests as distinct secondary peaks at higher energies. The elemental mapping (Figure 4b) concurrently displayed the presence of carbon and oxygen, measured at 9.18 mass% and 2.44 mass%, respectively. These minor elemental contributions were attributable to surface residues of the stabilizing agents (glycerol and ascorbic acid), which facilitated nanoparticle stabilization through established mechanisms involving hydrogen bonding and electrostatic interactions between their hydroxyl moieties and the SeNPs surface. Despite its presence, this capping layer appeared to be of insufficient thickness to entirely mitigate agglomeration, though it did not impart significant attenuation to the primary selenium X-ray emission.

HR-TEM analysis revealed the presence of spherical SeNPs with an average diameter of 3.9 nm (Figure 5a). The relatively narrow and homogeneous particle size distribution (Figure 5b) indicates that the synthesis process precisely controlled size growth, resulting in monodisperse SeNPs. SAED analysis (Figure 5c) displayed clear concentric diffraction rings, corresponding to the (101), (102), (201), and (112) crystal planes of selenium. This unequivocally proves that the SeNPs sample possesses a polycrystalline

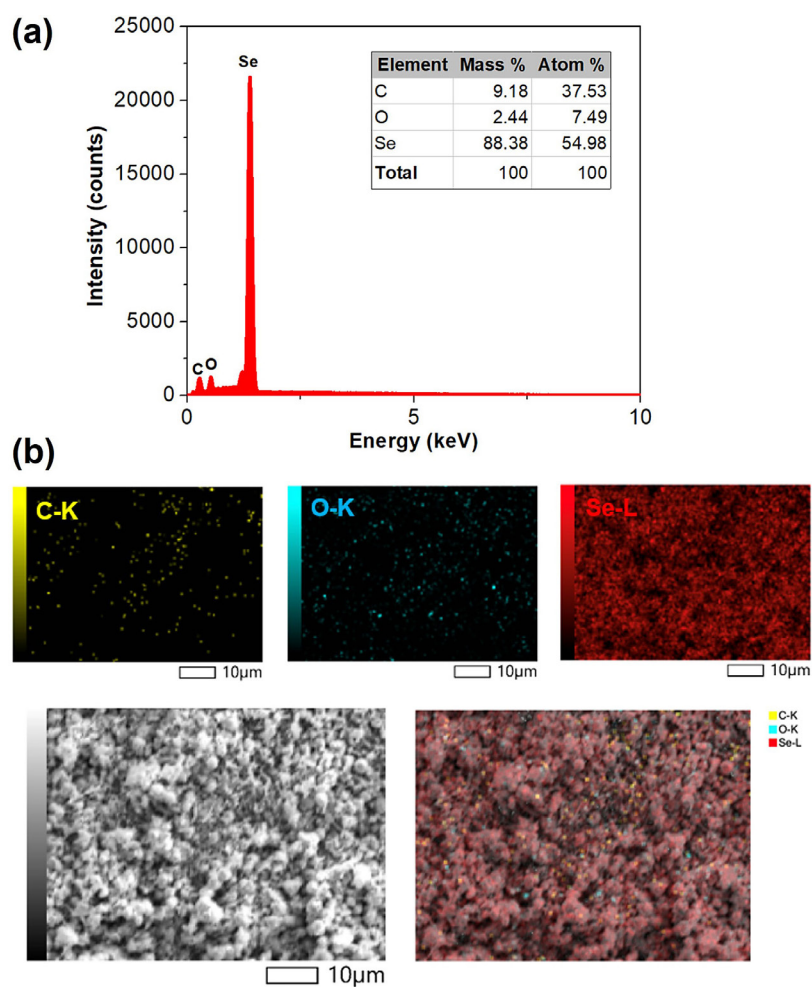


Figure 4. (a) EDX spectrum and (b) mapping analysis of solid SeNPs

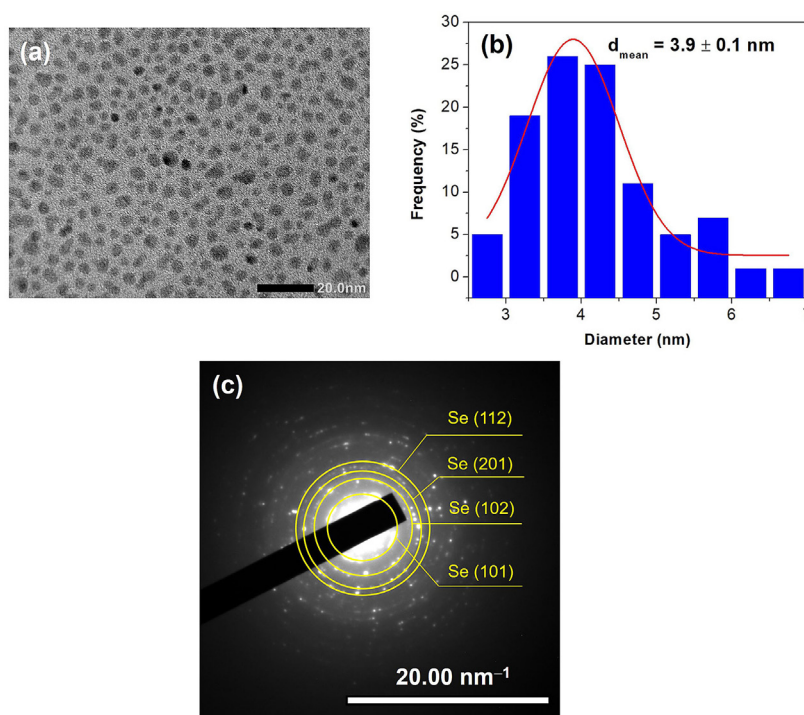


Figure 5. (a) HR-TEM, (b) particle size distribution, and (c) SAED analysis of SeNPs in glycerol

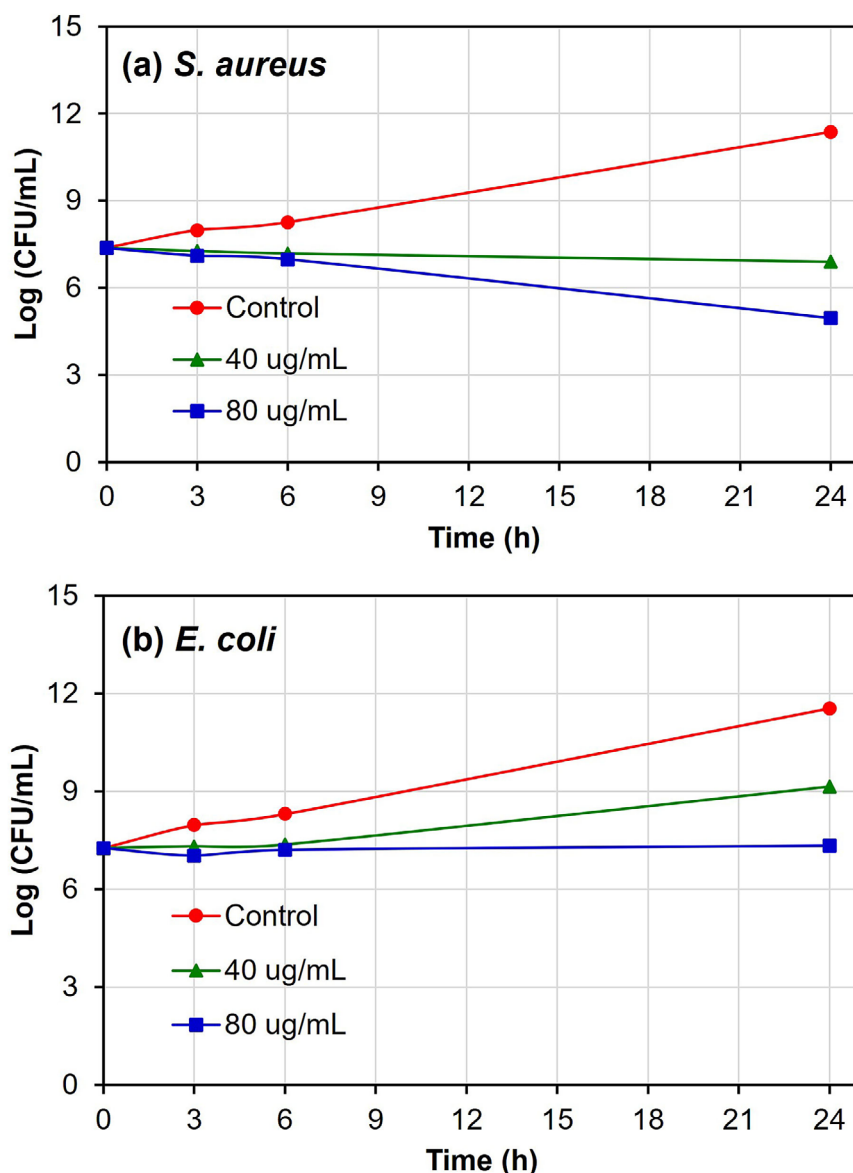


Figure 6. Growth curves of (a) *S. aureus* and (b) *E. coli* bacteria over time, treated with SeNPs in glycerol at various concentrations

structure with high crystallinity, consistent with the pure selenium phase found in earlier studies. The sharp diffraction rings further confirm that the grain size is sufficient to maintain crystalline order, preventing a transformation to an amorphous phase often seen with smaller grain sizes.

Antibacterial activity of SeNPs in glycerol

The growth inhibition of *S. aureus* and *E. coli* bacteria by glycerol-dispersed SeNPs was clearly demonstrated over 24 hours using the colony-forming unit (CFU) method (Figure 6). While the control group exhibited typical bacterial proliferation, with log(CFU/mL) values escalating from

approximately 7 to nearly 12, the SeNPs effectively suppressed growth. The antibacterial impact was notably concentration-dependent, with 80 $\mu\text{g/mL}$ proving highly effective against both gram-positive (*S. aureus*) and gram-negative (*E. coli*) bacteria. A concentration of 40 $\mu\text{g/mL}$, however, only managed to maintain or slightly reduce bacterial counts. This outcome supports existing literature highlighting SeNPs' ability to generate reactive oxygen species and compromise bacterial cell membranes (Huang et al., 2019; Zhang et al., 2021). Furthermore, glycerol's stabilizing and potentially enhancing properties (due to its moisturizing and osmotic effects) likely contribute to the observed antimicrobial activity.

CONCLUSIONS

This study details a straightforward and environmentally benign method for the synthesis of monodisperse, spherical SeNPs with an average size of 3.9 nm, directly within a glycerol matrix. The resulting colloidal SeNPs solution demonstrated stability over a minimum period of two months, a notable improvement when compared to SeNPs precipitated in water, ethylene glycol, or propylene glycol. This suggests glycerol's distinctive ability, likely attributed to its supra-molecular structure, to facilitate superior SeNPs dispersion. Importantly, the glycerol-dispersed SeNPs demonstrated significant inhibitory efficacy against the growth of both *S. aureus* and *E. coli* bacteria. The stabilizing and potentially synergistic properties of glycerol (owing to its moisturizing and osmotic characteristics) are hypothesized to contribute to the observed antimicrobial activity, thereby indicating considerable potential for their practical implementation.

Acknowledgements

We acknowledge Ho Chi Minh City University of Technology (HCMUT), VNU-HCM for supporting this study.

REFERENCES

1. Abdelsalam, A., El-Sayed, H., Hamama, H.M., Morad, M.Y., Aloufi, A.S., El-Hameed, R.M.A. (2023). Biogenic selenium nanoparticles: anticancer, antimicrobial, insecticidal properties and their impact on soybean (*Glycine max* L.) seed germination and seedling growth. *Biology*, 12(11), 1361. <https://doi.org/10.3390/biology12111361>
2. Bisht, N., Phalswal, P., Khanna, P.K. (2022). Selenium nanoparticles: a review on synthesis and biomedical applications. *Materials Advances*, 3, 1415–1431. <https://doi.org/10.1039/D1MA00639H>
3. Dang-Bao, T., Favier, I., Gómez, M. (2021). *Metal nanoparticles in polyols: bottom-up and top-down syntheses and catalytic applications*. In: K. Philippot, A. Roucoux (Eds), *Nanoparticles in Catalysis: Advances in Synthesis and Applications*. Wiley-VCH. <https://doi.org/10.1002/9783527821761.ch5>
4. Dang-Bao, T., Le, N.H., Lam, H.H. (2022). Tuning polyol-mediated process towards augmentation of zero-valent copper nanoparticles. *Chemical Engineering Transactions*, 97, 331–336. <https://doi.org/10.3303/CET2297056>
5. Dang-Bao, T., Nguyen, T.S., Tran-Dinh, N.T., Lam, H.H., Phan, H.P. (2023). Taking advance of isotropic-to-anisotropic morin-modified silver nanoparticles for simultaneous colorimetric sensing of trivalent chromium and iron ions. *Chemical Physics Impact*, 6, 100245. <https://doi.org/10.1016/j.chphi.2023.100245>
6. Ferro, C., Florindo, H.F., Santos, H.A. (2021). Selenium nanoparticles for biomedical applications: from development and characterization to therapeutics. *Advanced Healthcare Materials*, 10(16), 2100598. <https://doi.org/10.1002/adhm.202100598>
7. Huang, T., Holden, J.A., Heath, D.E., O'Brien-Simpson, N.M., O'Connor, A.J. (2019). Engineering highly effective antimicrobial selenium nanoparticles through control of particle size. *Nanoscale*, 11(31), 14937–14951. <https://doi.org/10.1039/C9NR04424H>
8. Huang, Y., Chen, Q., Zeng, H., Yang, C., Wang, G., Zhou, L. (2023). A Review of Selenium (Se) Nanoparticles: From Synthesis to Applications. *Particle & Particle Systems Characterization*, 40(11), 2300098. <https://doi.org/10.1002/ppsc.202300098>
9. Jamkhande, P.G., Ghule, N.W., Bamer, A.H., Kallaskar, M.G. (2019). Metal nanoparticles synthesis: An overview on methods of preparation, advantages and disadvantages, and applications. *Journal of Drug Delivery Science and Technology*, 53, 101174. <https://doi.org/10.1016/j.jddst.2019.101174>
10. Karthik, K.K., Cheriyan, B.V., Rajeshkumar, S., Gopalakrishnan, M. (2024). A review on selenium nanoparticles and their biomedical applications. *Biomedical Technology*, 6, 61–74. <https://doi.org/10.1016/j.bmt.2023.12.001>
11. Lian, S., Diko, C.S., Yan, Y., Li, Z., Zhang, H., Ma, Q., Qu, Y. (2019). Characterization of biogenic selenium nanoparticles derived from cell-free extracts of a novel yeast *Magnusiomyces ingens*. *3 Biotech*, 9, 221. <https://doi.org/10.1007/s13205-019-1748-y>
12. Ly, M.T., Dang-Bao, T., Nguyen, M.T.K., Lam, H.H., Tran, T.K.A., Phan, H.P. (2024). Exploring a surface-capping role of carboxymethyl cellulose for the synthesis of silver nanoparticles via the induction period in a catalytic hydrogenation. *Journal of Molecular Structure*, 1309, 138274. <https://doi.org/10.1016/j.molstruc.2024.138274>
13. Mollania, N., Tayeb, R., Narenji-Sani, F. (2016). An environmentally benign method for the biosynthesis of stable selenium nanoparticles. *Research on Chemical Intermediates*, 42, 4253–4271. <https://doi.org/10.1007/s11164-015-2272-2>
14. Nguyen, V.H., Lam, H.H., Nguyen, M.T.K., Do, T.A.S., Phan, H.P., Dang-Bao, T. (2025). A clear-cut synthesis of silver nanoparticles using glycerol as a multipurpose medium toward catalytic hydrogenation and antibacterial. *JCIS Open*, 19, 100141.

- <https://doi.org/10.1016/j.jciso.2025.100141>
15. Phan, H.P., Tran, C.G., Tu, Q.D., Nguyen, M.T.K., Lam, H.H., Tran, U.P.N., Dang-Bao, T. (2023). Making PVA-based antimicrobial food packaging film: an incorporated association with AgNPs-immobilized cellulose nanospheres. *Chemical Engineering Transactions*, 106, 235–240. <https://doi.org/10.3303/CET23106040>
 16. Phan, H.P., Nguyen, T.T.N., Hua, T.K.C., Tu, Q.D., Nguyen, M.T.K., Lam, H.H., Tran, T.K.A., Dang-Bao, T. (2024). *Musa paradisiaca* L. peel extract-bioinspired anisotropic nano-silver with the multipurpose of hydrogenation eco-catalyst and antimicrobial resistance. *Heliyon*, 10(16), e36037. <https://doi.org/10.1016/j.heliyon.2024.e36037>
 17. Puri, A., Mohite, P., Ansari, Y., Mukerjee, N., Alharbi, H.M., Upaganlawar, A., Thorat, N. (2024). Plant-derived selenium nanoparticles: investigating unique morphologies, enhancing therapeutic uses, and leading the way in tailored medical treatments. *Materials Advances*, 5(9), 3602–3628. <https://doi.org/10.1039/D3MA01126G>
 18. Ranjitha, V.R., Rai, V.R. (2022). Actinomycetes mediated microwave-assisted synthesis of nanoselenium and its biological activities. *Particulate Science and Technology*, 41(6), 904–914. <https://doi.org/10.1080/02726351.2022.2159899>
 19. Siddique, M.A.R., Khan, M.A., Bokhari, S.A.I., Ismail, M., Ahma, K., Haseeb, H.A., Kayani, M.M., Khan, S., Zahid, N., Khan, S.B. (2024). Ascorbic acid-mediated selenium nanoparticles as potential antihyperuricemic, antioxidant, anticoagulant, and thrombolytic agents. *Green Processing and Synthesis*, 13, 20230158. <https://doi.org/10.1515/gps-2023-0158>
 20. Thach-Nguyen, R., Lam, H.H., Phan, H.P., Dang-Bao, T. (2022). Cellulose nanocrystals isolated from corn leaf: straightforward immobilization of silver nanoparticles as a reduction catalyst. *RSC Advances*, 12(54), 35436–35444. <https://doi.org/10.1039/d2ra06689k>
 21. Tran, Q.H., Phan, H.P., Lam, H.H., Nguyen, P.T.D., Do, T.A.S., Tran, T.K.A., Dang-Bao, T. (2025). Glycerol-made ultrasmall platinum nanoparticles dispersed on eggshell-derived hydroxyapatite as a stable and superior reduction catalyst. *Results in Engineering*, 26, 105523. <https://doi.org/10.1016/j.rineng.2025.105523>
 22. Tripathi, N., Goshisht, M.K. (2022) Recent Advances and Mechanistic Insights into Antibacterial Activity, Antibiofilm Activity, and Cytotoxicity of Silver Nanoparticles. *ACS Applied Bio Materials*, 5(4), 1391–1463. <https://doi.org/10.1021/acsabm.2c00014>
 23. Ullah, A., Yin, X., Wang, F., Xu, B., Mirani, Z.A., Xu, B., Chan, M.W.H., Ali, A., Usman, M., Ali, N., Naveed, M. (2021). Biosynthesis of Selenium Nanoparticles (via *Bacillus subtilis* BSN313), and Their Isolation, Characterization, and Bioactivities. *Molecules*, 26(18), 5559. <https://doi.org/10.3390/molecules26185559>
 24. Xiao, X., Deng, H., Lin, X., Ali, A.S.M., Viscardi, A., Guo, Z., Qiao, L., He, Y., Han, J. (2023). Selenium nanoparticles: Properties, preparation methods, and therapeutic applications. *Chemico-Biological Interactions*, 378, 110483. <https://doi.org/10.1016/j.cbi.2023.110483>
 25. Zhang, H., Li, Z., Dai, C., Wang, P., Fan, S., Yu, B., Qu, Y. (2021). Antibacterial properties and mechanism of selenium nanoparticles synthesized by *Providencia* sp. DCX. *Environmental Research*, 194, 110630. <https://doi.org/10.1016/j.envres.2020.110630>